Handbook of Porous Solids

Edited by F. Schüth, K. Sing, J. Weitkamp

Surface Composition and Structure of Active Carbons

R. Schlögl

Department of Inorganic Chemistry, Fritz-Haber-Institute of the MPG, Faradayweg 4-6, 14195 Berlin, Germany

* Corresponding author: e-mail asek@fhi-berlin.mpg.de, phone +49 30 8413 4404, fax +49 30 8413 4401

1. The electronic structure of carbon surfaces

The element carbon occurs in a wide range of porous and non-porous forms. The preparative aspects and the utilisation of the pore structure have been discussed elsewhere. In this chapter the local chemical properties of carbon at chemisorption sites will be considered.

The chemistry of the element carbon is complex with a wide form of macroscopic and nanostructured varieties exceeding the historic definition of dual allotropes of graphite and diamond[1,2,3]. A simplified ordering scheme is given in Figure 1.

As in molecular organic chemistry, carbon occurs in sp^2 or in sp^3 atomic hybridisations in its elemental forms. The existence of sp carbon solids is still unclear and of no present relevance. The surface chemistry is strongly correlated to the chemical bonding within the bulk of carbon. Thus the main features of this bonding need consideration to understand the systematics of the surface chemistry of carbon.

The sp^2 configuration [4] of carbon atoms leads to planar graphene layers if only the most stable geometric arrangement of six-membered rings are formed as primary structural motif. The result is a family of well-ordered or turbostratically (randomly around the surface normal rotated graphene layers) disordered stacks of planar layers (graphene) with lateral dimensions ranging from a few nm to several ten micrometers. Graphitic and carbon black materials result from this arrangement. If the primary synthesis conditions are chosen such as to allow also the existence of less-stable non six-membered rings (NSMCR), strained 3-dimensional varieties of sp^2 carbon[5] such as fullerenes, nanotubes and carbon onions result. The strain (deviation form planarity) increases significantly the reactivity and

forces the ideally delocalised pi electrons from the sp² bonds into localised states ending in fullerenes in a poly-olefinic rather than in an aromatic electronic structure. Figure 2 illustrates this behaviour and indicates that for larger carbon units which may accommodate locally differing strain energies (or curvatures) a whole spectrum of double bond chemical reactivity will result.

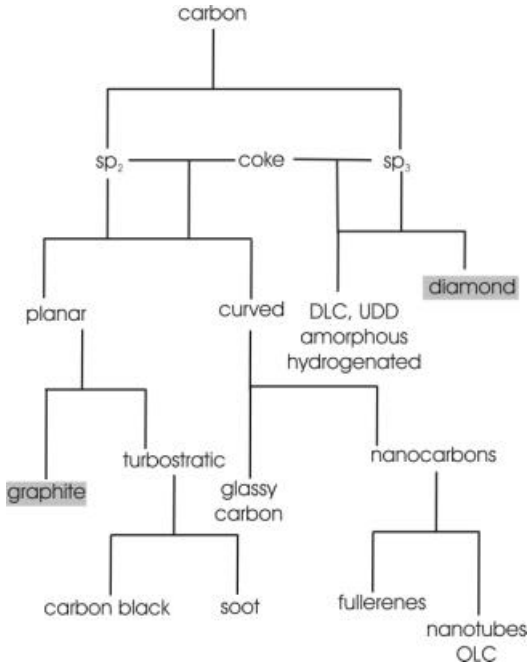

Figure 1: Families of polycrystalline carbon materials relevant for surface chemistry . Abbreviations: DLC: diamond-like carbon, UDD: ultradisperse diamond, OLC: onion-like carbon.

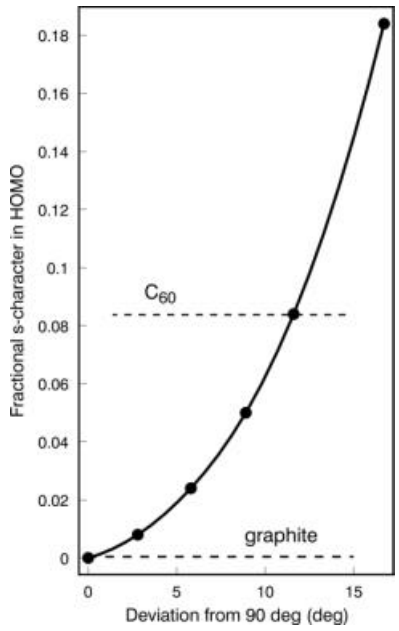

Figure 2. Fractional variation of the s-character of a sp² bond with increasing deviation from planarity. The bending occurs perpendicular to the direction of the sp² pz orbital. HOMO: highest occupied molecular orbital.

This is a fundamental insight into the fact that a vast variation in carbon functional group properties will result as soon as structural deviations are allowed from planar geometries. For bent sp² carbons all atoms at the surface are potential binding sites for heteroatoms.

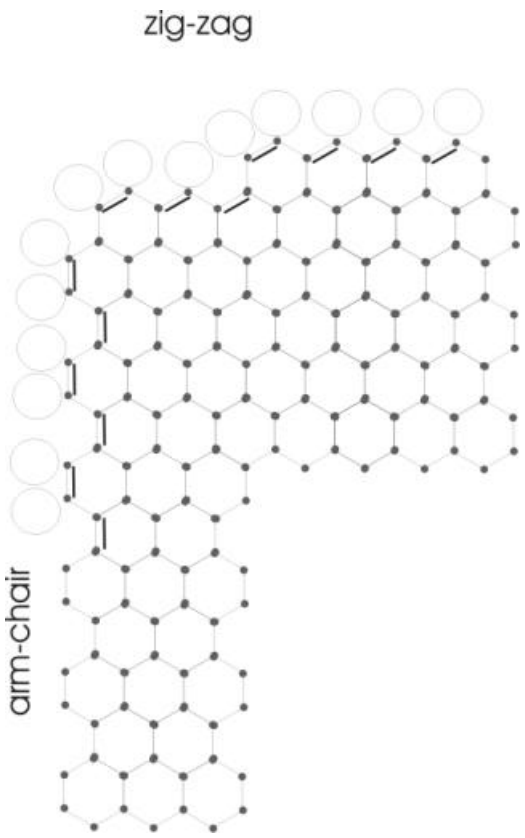

Figure 3. Prismatic terminations of a graphene layer. Despite the local chemical identity of all sites the space available for large and small surface functional groups is different on the two terminations as indicated by the circles.

For planar sp² carbons only two types of anchoring points exist with the well known zig-zag and arm-chair configurations. These two classical terminations of graphene layers are schematically shown in Figure 3. The zig-zag termination allows for an alternation of the ligand sites (top of Figure) whereas at the arm-chair faces double sites interchange with double empty sites. At corners mixtures of the two topologies occur. For non-hydrogen heteroatoms the topology thus has significant implications on the resonance stabilisation of carbon heterobonds with the “aromatic” pi-electronic system.

The most important point in the surface chemistry of carbon is the fact that due to the semimetallic or “aromatic” chemical bonding of the sp² configuration no functional chemistry can occur on the vastly dominating basal planes at the surface of the graphitic materials. All these sites are coordinatively saturated and can only act as nucleophiles or metals towards weakly adsorbing species. The surface chemistry of sp² carbon involving covalent bond formation is thus completely dominated by *defect sites* [6,7,8] to which the prismatic face boundaries of graphene layers also have to be

counted. As defects in a solid are extrinsic properties depending on the kinetic pre-history of the solid, no uniform nor predictable surface chemistry of a carbon variety is possible. The surface chemical properties of one and the same sample of a carbon material can be varied greatly by changing the defect structure (see below, e.g. Figure 8). Inversely, the surface chemistry of a carbon is an excellent marker for the defects present at the surface of the solid.

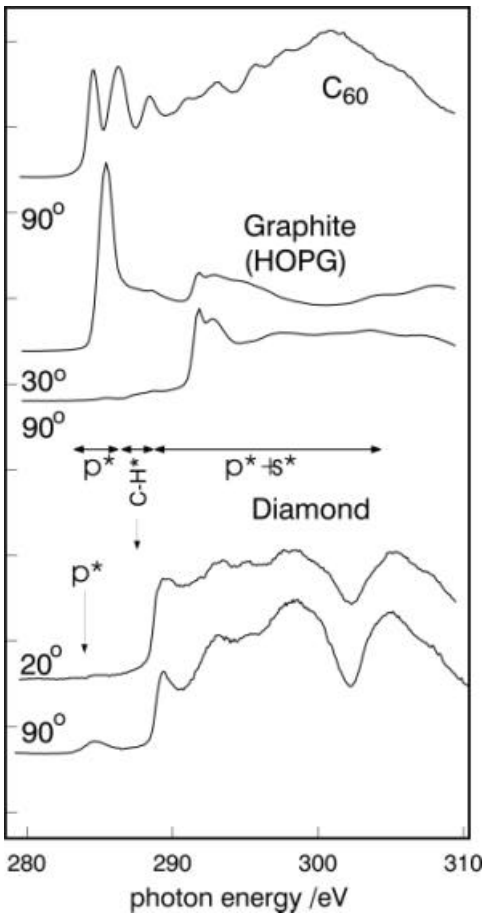

Figure 4: NEXAFS spectra for typical carbon materials. The data are obtained in UHV for thin films using polarised synchrotron radiation of energies given in the abscissa of the figure. The intensity is proportional to the density of unoccupied states.

The chemical anisotropy of typical carbon materials is reflected in their local electronic structure [9,10]. This property is probed with a maximum resolution by the surface-sensitive X-ray absorption fine structure spectroscopy [11] of the carbon K-edge [12]. Figure 4 summarises typical results. The local density of unoccupied states (beginning with the LUMO at lowest energies in the Figure) is probed in angular resolved form (for graphite and diamond films). The strongly bent sp^2 carbon fullerene C_{60} exhibits the electronic structure of a poly-olefinic molecule with well-resolved molecular resonances for the anti-bonding pi* states. Graphite as planar sp^2 carbon exhibits at similar energies than fullerene its metallic pi* conduction band. The skeletal sigma* bonds of the sp^2 hybridisation are well separated from the pi* states and occur at almost 10 eV higher energies. In the gap between pi* and sigma* states the anti-bonding states of C-H terminating bonds can be resolved. They occur as distinct feature in the diamond spectra which exhibit their main intensities near the energy positions of the sigma* bonds in graphite. The small pi* resonance in the diamond films is the signature of some graphite which is present as a layer parallel to the outer surface of the film sample. The presence of oxygen heteroatoms which have been removed for these reference experiments would lead to a reduction in intensity of the pi* resonances and cause a diffuse contribution to the deep lying sigma* states with both signatures being barely detectable

The sp^3 bonding configuration leads to 3-dimensional isotropic connections of tetrahedral carbon atoms[9,13,14]. The resulting ultra-stable structure is that of diamond. Its surface is terminated usually by hydrogen atoms resembling a macroscopic alkane molecule as shown in the data of Figure 4. Such surfaces are chemically very inert and require strong chemical reagents to change the terminating heteroatom. This process is so non-selective that over-oxidation and local thermal effects lead to an interconversion of the surface of diamond into graphite [15] on which the functional groups, characteristic of bulk graphite can all exist. This graphite impurity being well-ordered with respect to the bulk diamond is seen in its spectral signature in Figure 4.
Microporosity [16] in all these materials will result from chemical damage of the planar or bent graphene layers. If clusters of point defects [17] are present, then only short-ranged pores (etch pits) with low mechanical and chemical stability will result. If, however, some of the perimeter carbon atoms of such initial pores change their hybridisation from sp^2 to sp^3 and allow for an interlayer linkage, then stable and thus long-ranging primary pores can result.

Most of these pores are generated by chemical etching during carbon synthesis, purification or in deliberate post-synthetic processing. This etching starts at point defects [18,19] and enlarges them in a layer-by layer fashion. Their complex geometry [20] has been discussed elsewhere in this monograph, for the purpose of the surface chemical aspects it is sufficient to consider pore walls as a mixture of prismatic faces with stable C-H terminated sp^3 sites. The size of the pore will determine the abundance of sites for bulky terminal groups and hence affect the reactivity pattern of the inner surface.

Table 1 Some properties of model carbon substances

Property	FL-101	P40	FW-1	AF
Type	Flame black	Furnace black	Gas black	Graphite
Surface area (m2/g)	18	80	276	11
Particle size (nm)	95	29	13	1000
C at%	98,92	96,89	94,42	99,99
O at%	0,43	2,19	5,79	0.01
H at%	0,43	0,75	0,55	------
pH	7,2	8,5	3,2	7,1
Toluene extract (wt%)	0,1	0,15	0,06	------

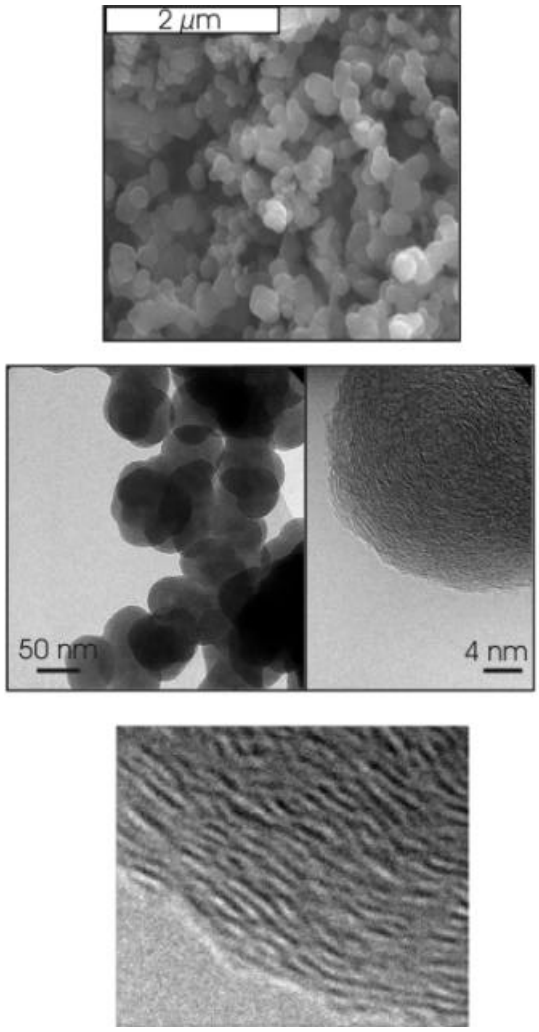

Figure 5: SEM (top) and HRTEM (bottom) images of carbon black revealing spherical secondary and primary structures (centre right and bottom). Note the difference in dimension. The bottom high resolution image reveals the turbostratic array of rather irregular graphene basic structural unity making up the spherical carbon particle shown in the centre left image. The blurred occurrence of some of the basic structural units occurs due to slightly differing tilt angles relative to the electron beam indicating a non-perfect layer stacking.

The surface chemical properties of common carbon materials with sp^2 basic structure are summarised in Table 1. These materials are commercially available and can serve as benchmarks for testing and development purposes. It is important to note that a vast number of black carbon materials has been developed for application in catalysts and other areas such as tyre manufacturing and pigment applications [21]. It is, however, not obvious to trace their application properties to any rationally observable surface property. For this reason a vast variety of black carbon materials is produced in bulk quantities with highly specific surface properties which are, however, mostly developed and controlled by purely empirical application-driven methods and not by a systematic surface structural classification. Similar observation hold for carbons used in coating or lubrication/friction applications. The origin of this still unsatisfactory state of surface analysis lies in the enormous width of surface chemical configurations possible on defect structures. In addition the methodology is not yet sufficiently developed to analyse all occurring surface groups with suitable chemical resolution.

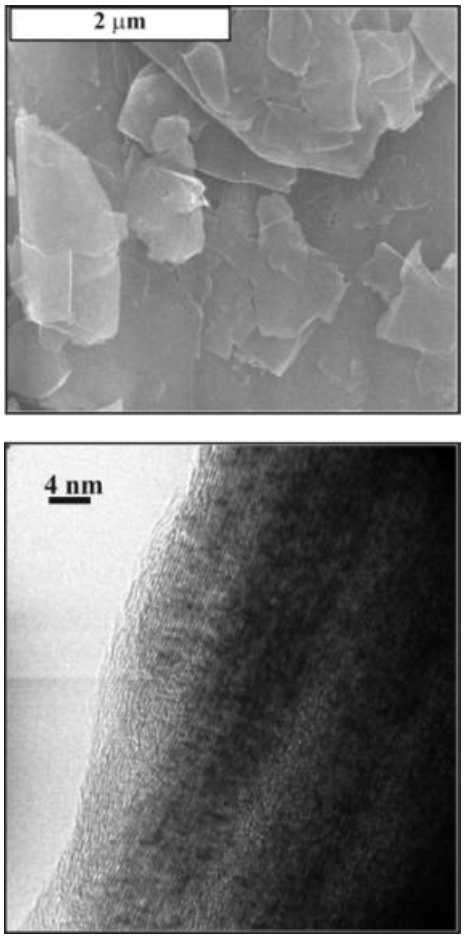

Figure 6: SEM (top) and HRTEM (bottom) images of natural graphite. The graphene layers are mesoscopic in size and stacked as parallel sheets to form the platelet mosaic structure of graphite flakes. The internal interface area and the surface area ratio prismatic:basal planes are drastically reduced as compared to microstructured carbons shown in Figure 5.

The chemical composition of the carbons described in Table 1 reveals that a significant fraction of non-carbon atoms exists in these materials. Most of them are in this type of non-coal materials (where heteroatoms belong to the skeleton of the basic structural units) bonded to the prismatic edges of the primary basic structural units. Only a tiny fraction of them is accessible at the outer surface and only a small fraction of those is chemically active (see below). The chemical composition is thus not a reliable indicator of the surface chemistry.

The presence of polar and charged, mostly oxygen-containing functional groups at the surface of the primary carbon particles (their sizes are given in Table 1) leads to

significant aggregation phenomena of carbon into secondary and tertiary structures [22] of frequently entangled strands of primary particles. These hierarchical structures create a large abundance of meso- and macro pore volume and form the basis of many application properties. The strength of the secondary structure in turn is strongly affected by types and abundance of functional groups. Figure 5 gives an impression of the tertiary structure (strands of spheres in SEM), of the secondary structure (spheres in TEM) and of the primary structure (spheres of basic structural units in HRTEM) [23,22]. The heteroatoms are located to a large extent at the boundaries of the basic structural units [24] occurring as defects in a hypothetical continuous graphitic carbon material. Most carbons prepared without the application of high temperatures (above 2000K) exhibit this structural principle. Graphitic carbons, on the other hand, are composed of comparatively large basic structural units forming piles of turbostratically disordered (random with respect to the in-plane structure) platelets. This much more compact and thus chemically homogeneous structure is depicted in Figure 6.
Many technical carbons and forms of adventitious carbons [25,26,27,28,29] are generated by incomplete combustion [30,31,32]. The polycondensation [33] occurring processes lead to the presence of polycyclic aromatic hydrocarbon and oxygen derivatives thereof. These molecules form an adsorbate layer which is usually about one monolayer thick. It can be removed by extraction with toluene or with trichlorobenzene. In the used solvent the polycyclic aromatic molecules can be analysed conveniently with GC-MS techniques. For many surface chemical applications it is desirable to remove this adlayer which interferes with the access of to the genuine carbon surface. High temperature inert treatment can lead to desorption of the aromatic molecules giving rise to a brownish film deposited at the cold locations of the apparatus used. If an oxidative treatment is considered the removal of the adlayer may be omitted as during the treatment most of the adlayer is carbonised to black carbon.

2. The generation of oxygen surface functional groups

The generation of oxygen functional groups can be considered as a preparation of intermediate states of the oxidation process of carbon to CO/CO_2 [34]. In most cases some of the carbon will be lost in the preparation process. All carbon forms are metastable against exposure to oxygen-containing gases and against oxidising agents such as nitric acid, sulphuric acid, hydrogen peroxide etc. These reagents and gases like di-oxygen, ozone, nitric oxide, CO_2 and [35] steam can all be used to create oxygen functional groups. Exposure of clean carbon to any of these reagents will also adventitiously create oxygen functional groups [36].
All oxidation reactions occur in two steps [37]. One of these is the reductive activation of the reagent producing an oxygen di-anion.

$$[C_x] + R\text{-}O \rightarrow [C_x]^{2+} + O^{2-} + R \qquad (1)$$

This can either occur by chemisorption and reductive dissociation at the basal planes of sp^2 carbon [38,39], or by direct activation of a radical centre formed by a dangling bond of an sp^2/ sp^3 carbon atom at the surface. As these centres are very reactive they will only be present after aggressive activation [40] of carbon in extremely inert environements (UHV, ultra-pure inert gases) or during in-situ gasification and during formation of solid carbon from atomic carbon sources. Schematically [41,42,43] the direct activation reaction occurs like:

$$\text{-C*} + O2 \rightarrow \text{-C-O} + O^* \qquad (2)$$
$$\text{-C-C} + O^* \rightarrow CO + \text{-C*} \qquad (3)$$
$$\text{-C-C-O} + O^* \rightarrow -CO_2 + \text{-C*} \qquad (4)$$

The regular case for chemical modification of carbon by oxygen will be the adsorption-reduction sequence [44,45]. For the common case of di-oxygen as reagent the process occurs like follows:

$$C_{basal} + O2 \rightarrow C\text{-}O_{2ads} \qquad (5)$$
$$C\text{-}O_{2ads} + 2 \text{ electrons} \rightarrow C\text{-}O_2{}^{2-}{}_{ads} \qquad (6)$$
$$C\text{-}O_2{}^{2-}{}_{ads} + 2 \text{ electrons} \rightarrow C_{basal} + 2\,O^{2-} \qquad (7)$$

The necessary electrons come from the conduction band of the graphite valence electrons. From this it is clear that neither diamond nor passivated carbons (hydrogenated, aromatic compounds adsorbed) nor the prismatic faces of sp^2 carbons are suitable substrates [46,47] for oxygen activation.
The second reaction is the diffusion of the activated oxygen di-anion to a site of covalent bond formation which must be a prismatic edge/defect site in sp^2 carbons. In strongly bent carbons of fullereneoid structures [48,49] this site may also be a localised double bond at the curved graphene sheet where an epoxide ring structure is formed.
When the initial C-O bond is formed several possibilities exist [50,51] of further reaction which are controlled by the boundary conditions and the reaction kinetics:
At too high temperature the C-O complex will desorb as CO
At too high temperatures and under excess of activated oxygen a CO2 group will form and desorb as carbon dioxide.
At intermediate temperature a carbon oxygen group with low disturbance of the graphene will form.
At very low temperature a complex carbon oxygen group with strong disturbance of the graphene layer will form.

The presence of other heteroatoms such as hydrogen, protons or nitrogen (from the oxidising reagents or in the gas phase) will allow for complex functional groups such as hydroxyl groups or N-O functions [52,53].
It occurs that reaction temperature and abundance of activated oxygen (partial pressures) are important parameters determining the chemical nature of resulting functional groups as well as the specific ease with which a given carbon-oxygen functionality is formed. This renders it clear that on structurally inhomogeneous surfaces (prismatic faces and defects) a wide variety of functional groups will begin to exist as soon as the reaction temperature is too low to permit

gasification and thus clean-up of the rough surface. This is illustrated by the data summarised in Figure 7 of functionalising some carbons described in Table 1 with hydrogen peroxide.

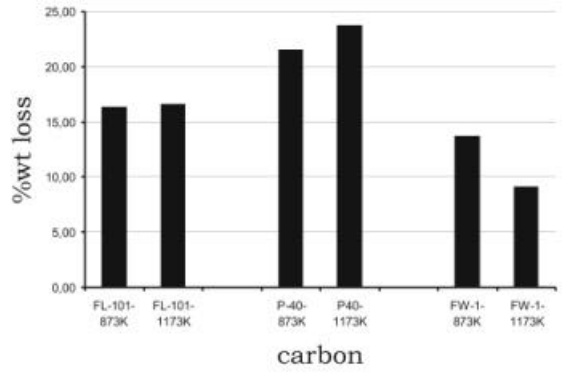

Figure 7. Weight loss of carbons after oxidation with aqueous hydrogen peroxide at 300 K for 24 h. Samples were pretreated with ammonia at the temperatures given to etch free a clean surface.

It occurs immediately that functionalisation removes a significant fraction of the carbon mass. It further can be seen that the removal does not scale with geometric surface as the sample with the highest specific surface area exhibits the lowest weight loss. Data like in Figure 7 may be used to probe samples for their specific defect density. The number of defects is sensitively related to the pre-treatment of a sample (here with ammonia) as can be compared with the P40 and FW-1 materials. Different carbon materials of the nominally same type "carbon black" (see Figure 1) which are both amorphous according to conventional wide-angle X-ray diffraction analysis exhibit significant microstructural differences manifesting in varying chemical reactivity.

Carbons functionalised to a high extent sometimes referred as "graphite oxides" [54] or which have been exposed to reactive gases at low temperatures exhibit a high reactivity. They may even spontaneously explode or burn in air and require very careful handling. Typical materials are samples after treatment with NO or ozone and hydrogen peroxide when they were not heated above 473 K during the functionalisation process. The fact that all oxygen functions are intermediates to gasification renders all such surfaces metastable. Freshly made materials are air-sensitive and change their properties in moist air and in water. Changes in weight, heat evolution or the formation of organic compounds in water (can go until the dissolution of the carbon [55] into highly coloured oxo-substituted molecules or humic acids) are drastic signs of this instability. Poor analytical reproducibility of their reactivity with continuing storage in air is very common.

3. The structure of carbon-oxygen functional groups

The surface chemistry of carbon is dominated by the consequences of oxygen bonding to free defect sites. A large number of sp^2 defect sites and of most sp^3 defect sites are saturated by hydrogen atoms [56] which can be identified as alkane desorbing at temperatures above 1400 K. These passivated hydrogenated sites [57,58] play, however, no significant role in the surface chemistry. They provide together with the basal graphene surface parts the origin for hydrophobicity of carbons.

Most carbon samples which were prepared by combustion techniques or have been exposed after synthesis to ambient air carry a sufficient number of carbon-oxygen functions that a significant interaction with polar molecules occurs rendering them hydrophilic and allowing for aggregation to complex superstructures (see Figure 5). The extent of hydrophilic interaction will depend on the abundance and chemical constitution of the carbon-oxygen functions which is determined by the local defect density of the carbon. Consequently, on a single particle a significant local variation of binding properties can occur. The overall hydrophilic character of a macroscopic sample is thus no indication of a homogeneous distribution of uniform surface functional groups. Overall hydrophobic carbons can be prepared by functionalising carbon oxygen groups with hydrophobic groups or by complete reductive hydrogenation of the surface.

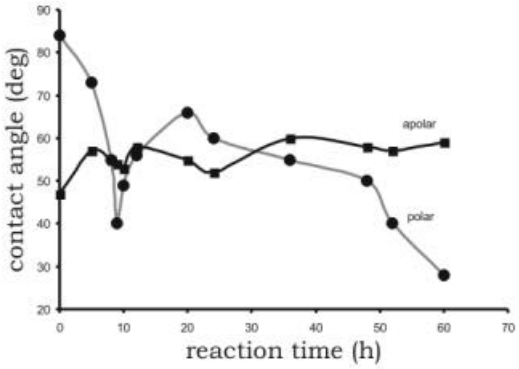

Figure 8: Contact angle measurements on highly graphitic carbon fibres with probe molecules water for hydrophilic and di-iodomethane for hydrophobic character. Plotted on the ordinate is the angle between the carbon surface and a droplet of the test liquid observed by a microscope as measure of the wetting behaviour of the test liquid . The parameter is the oxidation time in concentrated nitric acid at 343 K.

An example illustrating the heterogeneous nature of a carbon surface which was modified to increase its hydrophilic character is shown in Figure 8. A sample of carbon fibres (planar sp^2 carbon type) was treated with concentrated nitric acid to maximise its content of polar oxygen groups. With reaction time it was not possible to remove the hydrophilicity of the sample which is sensed by the contact angle in di-iodomethane, as the basal plane abundance was not changed with this treatment. The hydrophilic surface function changed, however, significantly in abundance and character with time of reaction giving rise to the strong modification of the water contact angle. Only after excessive oxidation

the hydrophilic character wins over the hydrophobic property. The data indicate clearly the co-existence of apparently incompatible chemical functions on solid surfaces which are usually locally heterogeneous and thus can host a wide spectrum of chemical functions which exclude each other in homogeneous systems.

The carbon oxygen surface functions can be distinguished in two large groups; one is chemically active and will act as solid acid-base systems [59,60,61], whereas the other group is chemically inactive.

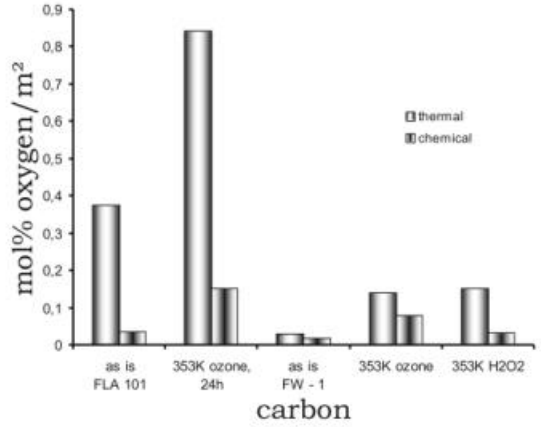

Figure 9: Abundance of oxygen atoms in mole/m² for two carbon materials after oxidation with ozone/hydrogen peroxide. "Thermal" denotes all oxygen from integral temperature-programmed desorption of CO/CO2 up to 1173 K, "chemical" denotes all acid function neutralised with 1n NaOH.

Chemically inactive oxygen groups occur in temperature-programmed desorption experiments as high-temperature species at above ca. 773 K terminating the desorption only well above 1200 K. These species are numerous on surfaces of carbons prepared by combustion methods (technical carbon blacks, activated carbons). They interfere with spectroscopic or temperature-programmed analysis of the chemically active oxygen functions and have to be taken into account in all quantitative evaluations [62,63]. The chemically inactive functions may play a major role as intermediates and/inhibitors in carbon oxidation processes. A quantitative determination of the relative abundance can be obtained from comparison of the total oxygen desorbing thermally and the sum of all oxygen species reactive in acid-base neutralisations. Figure 9 reports some data. The specific integral content of oxygen species per unit surface area is compared for two carbon black samples and two modification agents. The response of different microstructures to the same modification agent is strikingly different (factor of 2 for chemical active groups and factor of 4 for total oxygen content). Ozone is much more effective (roughly factor of 5) as gas phase modifier than hydrogen peroxide in aqueous solution at the same temperature. The difference between chemically active and total oxygen content is in all cases very significant and difficult to predict. The absolute storage capacity of oxygen on/in carbon is significant and underlines the metastable character of highly functionalised carbon samples.

The group of chemically active oxygen functions [64] is traditionally described according to their reactivity towards liquid water. The oxygen groups may behave as Broensted acids and increase the number of protons in water or they may act as solid bases and decrease the number of protons in water below the autoprotolysis equilibrium.

$$[C_xOH] + H_2O \; ? \; [C_xO]^- + H_3O^+ \qquad (8)$$
$$[C_yO] + H_2O \; ? \; [C_yOH]^+ + OH^- \qquad (9)$$

The efficiency with which a solid acid carbon shifts the autoprotolysis equilibrium of water is seen in the pH change measured after immersion of a specified quantitiy of carbon into demineralised water. Such data are given in Table 1. Solid carbon acids [65] exhibit similar strengths than strong organic acids (acetic acid) but less strong acidities than mineral acids. One sample reacts overall basic. The relative small apparent efficiency is, however, no measure for the strength of the acid functions on the carbon. For a single acid function the efficiency is given by

$$pH = ½ (pk_s - \log [conc.]) \qquad (10)$$

with pk_s denoting the dissociation constant which is a measure for the strength of an acid function. If the abundance of structurally identical acid sites is determined then one could conclude about the acid strength. For carbons, however, this is not possible as not a single acidic function is present but a wide variety of oxygen functionalities with vastly differing structures and hence pks values. The observed pH change is thus the sum over all the species times their relative abundancies. The data in Table 1 show that on a single carbon acidic and basic functions can co-exist allowing for the fact that even large amounts of strongly active oxygen functional groups will not change much the pH of water as they compensate each other according the equations (8) and (9).

Recommendation: Determination of the pH change of functionalised carbon materials. 1m² of sample (equivalent to 10-100mg material) is weighed into a Schlenck flask prefilled with Ar. Under Ar flushing 50.0 ml of bi-distilled water degassed under Ar and temperature-adjusted to 300 K is added. After intensive shaking for 20 min an aliquot of the water is removed and analysed for its pH value using a precision-calibrated pH meter. The pH change is determined against a blind determination using the exactly same procedure but without the carbon sample being present.

The knowledge about chemical structures of functional groups stems mostly from chemical derivatisation experiments [66,1] backed by vibrational analysis of highly functionalised test samples. It is convenient to derive several archetypical structures of oxygen functional groups represented in Figure 10. Carboxylic and acid-anhydride functions (A,C) react most strongly acidic in water. As their structures contain the carbon dioxide molecular fragment

already as excellent and thermodynamically highly preferred leaving groups it is clear that these most reactive groups are also the least stable functions. Depending on the abundance and density of neighbouring groups desorption of carbon dioxide from these functions occurs from 300K up to ca. 723 K. The finestructure often seen in desorption traces may be indicative of the detailed local environment which can be more complex as indicated in Figure 10 F. Phenolic and carbonyl groups (quinoid structures if resonance stabilised with the aromatic pi electrons) (B,E) react only weakly acidic against water and require stronger bases than water for their safe identification. Reaction with carbonate or bicarbonate solutions under liberation of CO2 are suitable methods of determination. The thermal stability and thus their abundance is much higher than those of the strongly acidic functions. Thermal desorption leads to CO and requires temperatures up to 1273 K for complete removal. Lactones (D,F) and other ether functions react moderately acidic, in particular if they are adjacent to other oxygen functional groups.

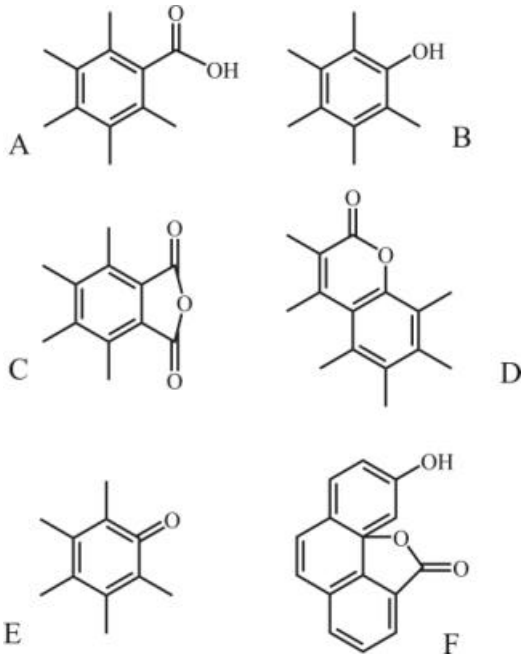

Figure 10: Schematic representation of the local chemical structures of chemically active oxygen functional groups: A:carboxylic acid, B:phenolic, C: acid anhydride, D: lactone, E:quinoid (carbonyl), F: complex lactone.

A basic reaction with water [67,68,69] occurs with quinoidic and “super-quinoidic” pyrone structures represented in Figure 11. Scheme A represents one possible quinoidic function with one oxygen atom in resonance stabilisation. Even more basic is the pyrone structure shown in Figure 11 B which exhibits two oxygen atoms in resonance stabilisation and one oxygen atom being incorporated into the graphene structure. This heterocyclic structure causes a severe perturbation of the graphene unit as can be seen from the cross-sectional model in Figure 11C revealing a deviation from planarity of the graphene unit. As many combinations of carbonylic oxygen atoms with heterocyclic oxygen atoms are possible, a whole family of pyrone structures is in existence. Chemical derivatisation reactions were used to unravel the existence of such synergistic structures leading to strong chemical reactivity against protons which may not be detectable in physical characterisation experiments looking at too local properties of single carbon-oxygen bonds (interpreted as single functions).

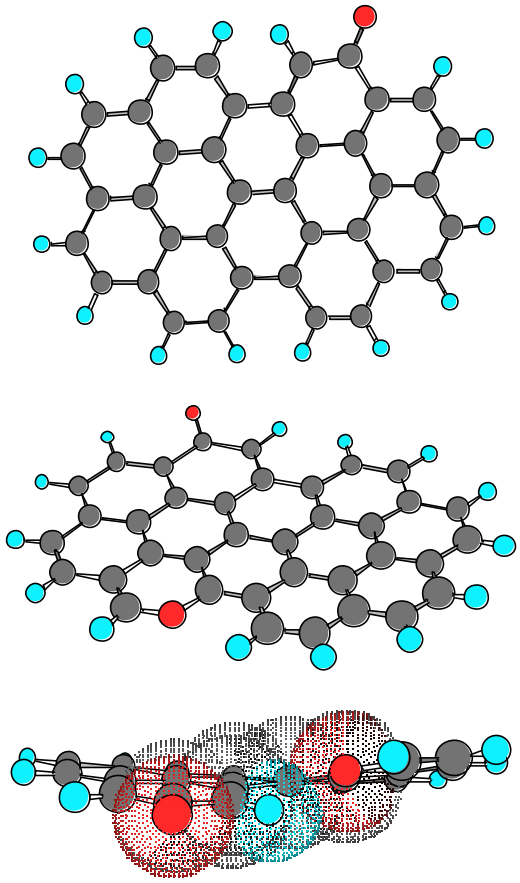

Figure 11: Schematic representation of Broensted-basic oxygen functional groups: A: a single oxygen atom forming a quinoidic structure, B: two oxygen atoms resonance stabilised in a pyrone structure, C: perturbation of a model graphene particle by incorporation of oxygen.

Table 2 Selected Properties of model oxygen functions on a hypothetical graphene fragment. All bond distances in pm.

Model group	Rel. heat of formation (%)	C=O	C-O	C-C C-C
Graphene	100	----	----	142 142
Carboxylic	40	123	136	150 139
Hydroxyl	91	----	136	139 145
Acid Anhydride	38	122	139	151 151
Carbonyl	82	121	----	152 126
Pyrone flat	92	124	139	147 136
Pyrone twist	60	224	138	146 136

The addition and incorporation of oxygen atoms into graphene units leads to severe disturbances of the finite electronic structure of such units. This was investigated by subjecting the model structures of Figures 10 and 11 to semiempirical quantum-chemical calculations using the AM-1 formalism. All additions of oxygen groups led to double bond localisations and hence to the disruption of the equal distribution of pi electrons resulting in alternating long and short carbon bonds in the vicinity of the perturbing oxygen atom. This in turn causes a de-stabilisation of the system recognised in the substantial lowering of the heat of formation parameter for the system. Typical data are given in Table 2. The data there further reveal that the pyrone unit which can artificially be held flat or may be allowed to twist the graphene layer is a particularly strong modifier of the electronic structure of the model graphene unit. The data further show the enormous propensity of the carbon-oxygen system to lower its energy by releasing pre-formed carbon dioxide units. The extensive double bond localisation for which fullerenoid structures are practical examples [70,71] further facilitates the addition of more oxygen species i.e. from activated di-oxygen in the form of oxiranes and other highly unstable structures supporting the oxidation of carbon. In this way it becomes clear that oxygen functionalisation is not only the preparation of gasification intermediates but is a destabilisation of the carbon support. It is obvious that the perturbed graphene units are also activated towards reaction with any other gas phase containing hetero-nuclear molecules (in catalytic applications such as hydrogenations for example). This has to be taken into consideration for all applications of functionalisation where thermal processing or operation at elevated temperatures in reactive chemical environments is considered. Typical cases for such applications are functionalisations for increasing the number of anchoring sites for reactive metal deposition in the synthesis of heterogeneous catalysts [72,73,74]or the surface activation of carbon used as filling and strengthening functional additives in composite materials [75,76,77,78].

It must be stressed that the structural classification of the oxygen groups is simplifying the facts significantly. First, the co-existence of structurally differing functional groups on electronically neighbouring sites (resonance stabilisation) will cause non-additive effects of chemical bonding and hence in reactivity (see the cases of pyrones in Figure 11 or complex lactones in Figure 10). Second, real surfaces are rough and exhibit a variety of carbon topologies in contrast to the model revealing homogeneous zig-zag termination. Third, there are unknown non-reactive oxygen species (see above) which interfere as neighbouring groups with the properties of the reactive groups (site isolators, polarisers). These effects are expected to lead to a wide spectrum of reactive properties and to a distribution [79] of e.g. pk_s values rather than to a defined surface acidity and stability. This expresses itself in infinite variations of thermal desorption profiles and in complex titration curve responses (see below). To give an impression of the chemical complexity and anisotropy of a carbon surface, Figure 12 presents a microparticle in top (A) and side views (B) with terminating atoms drawn in full relative size. The vastly different chemical "ligand character" of various locations on this small section of a real carbon particle speaks for itself and indicates the possibility of a virtually unlimited variation in chemical reactivity with varying kinetic parameters of the functionalisation reaction.

With all this complexity in mind the following recommendations are given as starting points for the preparation of functionalised carbons. With many laboratory experiments these procedures were found to be reliable and useful for generation of reproducible surface properties. Note that the structural details of a given carbon may lead under the conditions given to significantly different properties from those expected after the descriptions given. Very useful is a unifying pre-treatment of any carbon sample prior to surface modification. Two procedures besides radical graphitisation at temperatures above 1800 K are useful.

Recommendation: Simple pre-cleaning: Subject the sample to thermal annealing at 1173 K for 3-6 h under a carefully cleaned gas stream of He or Ar using gas velocities of about $1000h^{-1}$. The complete absence of any CO_2 evolution is the sign for completion of the cleaning . Cool to the desired temperature in a fast gas stream. Use clean and lined quartz tubes. Beware of free flying carbon dust. Allow for a large free volume in the tubular furnace and ensure leak-free connections to the gas supply (mind leaks at high temperature).

Recommendation: Inert pre-cleaning: Similar procedure as above with the addition of a treatment of the sample with 5% ammonia in inert gas at 873 K for 6-9 h followed by a cooling/flushing in inert gas. The product is stabilised against oxidation and may contain up to 5 at% nitrogen as pyridines, cyanides and N-H groups (abundant when not carefully flushed).

These pre-treatments may lead to up to 30% mass loss of the materials and to a slight loss in surface area. Fullerenoid structures will completely be converted into flat black carbons [80] as all NSMCR units will be lost. The pre-treated samples must be used within 24 h for functionalisation. They must never be brought in contact with air and may not be stored in plastic containers. These samples are highly reactive towards adsorption of polar and non-polar molecules (hydrocarbon impurities, plastic softeners, oil vapours etc).

A good practice for the following high temperature treatments is the determination of suitable temperatures by performing thermogravimetric pre-experiments in diluted oxygen and finding the temperature onset of bulk gasification. (use heating rates of 5K/min or less for this purpose).

Recommendation for creation of basic functional groups: a) simple: Expose pre-cleaned carbon immediately after cooling to 300 K (not at higher temperatures!) under inert gas to ambient air for 30 min. b) better controlled: reheat pre-cleaned carbon in a mixture of ethylene and oxygen (1:0.5 molar) diluted tenfold in inert gas by using space velocities of below $1000h^{-1}$. Suitable temperatures are 573-673 K, treatment times are 6 to 24 h.

Recommendation for acidic functional groups: a) high temperature: re-heat pre-cleaned carbon in 5% oxygen in inert gas to 673 K for 4 h and cool in oxygen flow; b) low-temperature method: immerse pre-cleaned carbon in 30% hydrogen peroxide and heat carefully to 353 K for 1 h. For very high surface area carbon this procedure is not recommended (rapid total oxidation!). In this case use concentrated nitric acid (not recommended for well-ordered carbon as graphite intercalation compounds will form and mechanical disintegration may occur).

These recommendations are to be understood as starting points for specific optimisation procedures. For reliable and reproducible results it is of paramount importance to control the partial pressure of oxygen in all steps and thus to be very careful with gas purities and leakage problems of the furnaces. Heating rates should not exceed 15 K/min in all procedures. Only a detailed analysis of the properties of the functional groups generated allows to optimise the carbon surface chemistry which may require a significant number of tests and strong deviations from the recommended starting treatment conditions. It has to be noted that all these treatments interfere with the pore structure of the carbon in difficult-to predict manners. A loss of microporosity due to preferred defect oxidation as well as creation of micropores by removal of "debris" in the particles will occur. If the pore size distribution is critical for an application, suitable tests need to be included into the optimisation procedure.

4. Analysis of carbon-oxygen functional groups

For any description or application of a carbon material the qualitative and quantitative analysis of its functional groups is essential [81,65,82]. The by far most relevant case is that of co-existing –H and –oxygen functions. This case will be considered in the following text. For –N, -S and-Hal functions the reader is referred to special publications [83,84].

Carbons from artificial sources or after high temperature treatment of natural precursors contain most of their bulk analytical heteroatoms in the form of functional groups. Examples of such data which can be obtained from combustion elemental analysis are given in Table 1. In the preceding sections it was emphasised that these numbers allow no conclusion of structure or even on chemical availability of the heteroatoms due to the enormous complexity of bonding situations. It was also made clear that only a small fraction of all heteroatoms is available for chemical reactions such as substitution or acid-base reactions. If the characterisation of this fraction is of relevance then only chemical analytical methods with probe reactions can be recommended as secure analysis strategy. These "old-fashioned" but extremely selective and accurate methods [69,85,86,87] may be supported by temperature-programmed desorption (for oxygen) and oxidation (for hydrogen groups) analysis. Surface analytical and vibrational spectroscopy may be used as further complements focussing on the average local structure and the surface electronic properties. Any functional classification of a carbon material based only on physical-analytical methods is, however, insecure and may lead to an incomplete description of the surface reactivity.

The chemical functional analysis should start with a pH test as described above and requires the knowledge of the surface area. For visibly hydrophobic samples wet chemical tests in aqueous media are very difficult and should be substituted by thermal analysis concentrating also on the observation of organic molecular desorbing species (aromatic compounds). Most practical samples which have been exposed to ambient air exhibit, however, a finite hydrophilic character which allows the application of wet chemical analysis.

A first overview of the properties of functional groups can be obtained from backtitration analysis of carbon with 0.1n and 1.0 n NaOH and HCl respectively. Typical data are exemplified in section 2 (Figure 9). These data imply that significant differences in reactivity must exist for different samples after identical treatments. Usually one needs to characterise the reactivity further. This can be done by analysing the sorption isotherms of various reagent onto the carbons. Besides HCl and NaOH also systems with less strong dissociation strengths are of great value. Typical systems are carbonate, phosphate, acetate and oxalate.

The functional groups depicted in Figure 10 may be quantitatively discriminated by the following series of selective neutralisation experiments which can be made quantitative by backtitration:

carboxylic acids: sodium hydrogen carbonate
carboxylic acids and lactones: sodium carbonate
carboxylic acids, lactones and phenolic groups: sodium hydroxide
carboxylic acids, lactones, phenols and carbonyls: sodium ethoxide

This list gives also an impression of what can be expected for any desired chemical reactivity from the various species of oxygen functional groups. It is further obvious that this distribution of reactivity may well lead to a heterogeneity of the support properties of carbons for e.g. metal particles [88]. When considering this, attention must be paid to the stability and hence availability issues discussed in the previous section.

Due to the much more elaborate experiments for quantitative determinations with the list of reagents quoted above, the vast majority of experiments limits itself to mineral acids and bases as reactants. These experiments are still time-consuming and elaborate. For this reason numerous attempts were made to exert a direct titration [59] of the carbon surface immersed in water. The method has the advantage of directly representing the distribution of pk_s values of the sample. Its great disadvantage is, however, the limited sensitivity (even with very sensitive detection instrumentation) and more severely the dependence on transport kinetics. Both the pore system and the immanent partly hydrophobic character of the graphene sheets render the equilibration of any liquid reagent with surfaces very slow.

This dependence of the neutralisation reaction on external and pore mass transport kinetics broadens the titration response and often completely prevents the application of this method. The replacement of wet chemical titration by microcalorimetric titration of gaseous bases and acids (such as ammonia, SO_2 and CO_2) is a useful but technically difficult and time-consuming solution [89].

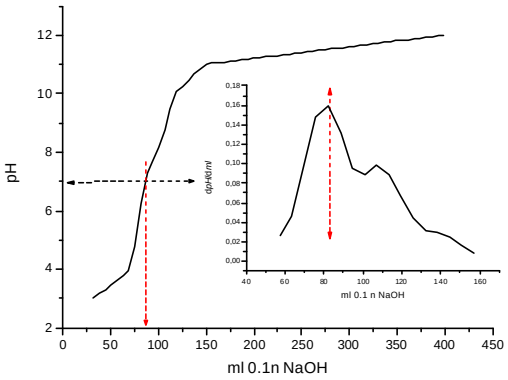

Figure 13: Direct titration experiment of surface acidity with 0.01 n NaOH. Sample: FW-1, treated with hydrogen peroxide at 364 K (see Table1 and Figure9).

In Figure 13 a successful direct titration experiment is shown using a highly functionalised carbon black. The titration curve reveals several unresolved steps pointing to a distribution of pk_s value in contrast to a pure oligo-basic acid (e.g. H_3PO_4) revealing a number of discrete signals equal to the number of dissociation steps with characteristic pk_s values. The derivative of the titration curve shows several maxima but reveals further a broad distribution of unresolved dissociation steps. The largest contribution to the distribution stems from strong acid sites as indicated by the equivalence point coinciding with the neutral point of the system. This is rather unusual for carbon surfaces and can be traced back to the very efficient functionalisation with hydrogen peroxide. The other maxima being shifted with their equivalence points into the basic regime of the system indicate the existence of weaker acidic sites giving rise to incomplete dissociation and hence to partial hydrolysis of their salts leading to the overall basic reaction.

In most cases this method of direct titration will, however, give unreliable results (show only the fraction of strongly reacting sites easily accessible at the outer surface of the sample) and must be used with reservation unless highly functionalised and strongly hydrophilic samples are to be investigated.

The most reliable and versatile method is the back-titration [90,69] with any reagent of choice. In this method the concentration of the adsorbent is varied in suitable steps allowing to probe the pk_s distribution in step functions. The data can be analysed in terms of the Langmuir adsorption model and can thus give indications about the acidity of the predominant active species. The experimental details of the back-titration are critical and will be given in the following recommendation.

Recommendation of a backtitration experiment. A series of 2x9 experiments has to be carried out. For concentrations of 0.0025, 0.005, 0.01, 0.025, 0.05, 0.1, 0.25, 0.5 and 1.0 normal reagents a set of sample and blind experiments must be prepared. All experiments must be carried out with strict exclusion of air (oxygen and CO_2) and should be done under Ar in Schlenck flasks. The water must be doubly distilled and carefully degassed from its boiling state by cooling in flowing Ar.

50 mg sample (less for surface areas above 250 m^2/g) are brought in contact with 50 ml reagent under Ar. After 24 h agitation of sample and blind experiments (after 6 hours only the outer surface groups have usually reacted) the flasks are allowed to stand for sedimentation. Highly functionalised carbons may partly dissolve and yield intensely coloured solutions of polycyclic oxygenates. A carbon-free aliquot is back-titrated with a suitable reagent. Great care must be exerted to reproducibly transfer the whole of the aliquot into the titration equipment.

The resulting adsorbed amount for each strength of reagent are analysed in terms of the Langmuir model:

$A/V = A/V_{mono} + [(1/b) x V_{mono}]$

With A = reagent concentration, V = adsorbed amount, V_{mono}, adsorbed amount for full coverage, b = sorption coefficient

A plot of A vs. A/V should result in a straight line allowing to estimate V_{mono} and b.

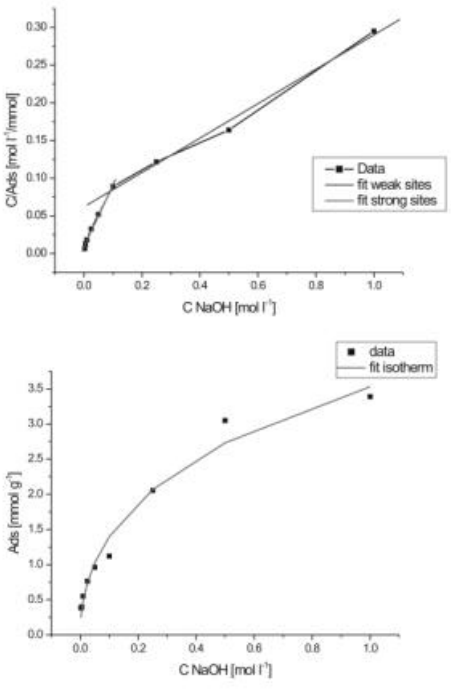

Figure 14: Results of a multiple backtitration experiment using the same sample as for the experiment described in Figure 13. The single Langmuir model fit resulted in a saturation coverage of 12 mmol OH/g and a sorption constant of 0.48 indicating rather strong adsorption sites (giving the first maximum in the direct titration of Figure 13). The linearised model allows clearly to add a second sorption isotherm involving much weaker acidic sites. The lack of data points

and the uncertainty about the real number of adsorption processes precludes a meaningful quantification of the site distribution.

The results of a multiple adsorption experiment are displayed in Figure 14. The amounts of adsorbed NaOH are plotted vs. the base concentration. The resulting curve may be fitted with a Langmuir adsorption model yielding an excellent agreement with data points at low concentrations. At intermediate concentrations some systematic deviations from the fitted line imply that a single adsorption isotherm is insufficient for the description of the adsorption process. This is in accord with the distribution of pk_s values and multiplicity of adsorption sites.
The linear representation of the Langmuir model in the bottom trace of Figure 14 clearly indicates by lines with different slopes and hence b-values the co-existence of two adsorption processes occurring on strongly acidic sites and on weakly acidic sites. The latter requires relatively high concentrations of adsorbent to become activated for chemisorption. It may be argued that even more than two processes may exist but their exact determination would require many more sorption experiments at high base concentrations. In this range of strong basicity care has to be taken not to intermix acid-base reversible neutralisation with irreversible hydrolysis processes destroying the sample surface.
Oxygen functional groups may also exhibit a redox-reactive behaviour [91]. Typically quinoidic structures may be redox-active in contact with multi-valent metal ions in solution. An overall quantification of this often neglected property of carbon surfaces can be obtained by reacting the sample with KI in non-aqueous solution (e.g. DMF).

$$3\ KI \rightarrow I_3^- + 2\ \text{electrons} + 3\ K^+ \qquad (11)$$

$$C_xO_y + 1\text{electron} + K^+ \rightarrow C_xO_y\text{-}K \qquad (12)$$

The amount of tri-iodide formed according to equation (11) can be determined by titration with sodium thiosulphate and gives an integral measure of the redox activity. The tri-iodide is very poorly adsorbed on the carbon and allows a reliable measurement. The choice of the solvent may be critical as reaction (11) contains an equilibrium between tri-iodide and free iodine which is well-adsorbed on many carbon surfaces.

A spectroscopic characterisation of OH groups can be done for highly functionalised samples by using vibrational methods [92,93,94] such as FT-IR or DRIFT experiments. The strongly absorbing nature of the sample renders the interpretation of spectra difficult. Great care must be taken to use very clean diluents (KBr) and a carefully background corrected spectrum. The vibrational bands and the assignment observed over a large number of samples are listed in Table 3. It occurs that carboxyl groups, carbonyl groups and phenol/lactone groups can be identified with this method. The relative abundance of the groups may be estimated from carefully determined band intensities. Estimations of surface abundances including the C-H vibration and OH valence modes should, however, not be done due to a number of adverse effects on the cross-sections and the interference of OH-vibrations with those from the KBr matrix.

Attempts to correlate the carbon vibrational bands with those of polyclyclic aromatic compounds are unsuccessful as the large structure and complex defect situations preclude the observation of many combination bands carrying the structure-specific information. All spectra of even large molecular model compounds are significantly more complex and richer structured as solid carbon spectra indicating that the functional groups are multiply isolated on a solid support and that the perception of carbon surfaces being approximated by molecules has to be seen with great care.

In porous samples of carbons significant amounts of gaseous or adsorbed carbon oxides give rise to sharp and characteristic bands at 2355 cm-1 (doublet) for CO2 and at 2045 cm-1 for CO.

Table 3 Vibrational bands commonly observed on oxo-functionalised solid carbons. Not all bands appear on each sample.

Position in cm^{-1}	Assignment	Description
3450 - 3430	-OH	Isolated valence
2920-2900	-C-H	Aliphatic valence at prism faces
1730	-C=O	Stretch of carboxyl groups
1720	-C=O	Stretch of lactones
1630	-C=O	Stretch of isolated carbonyl
1618	-C=C	Localised double bond
1608-1585	-C=C, -C=O	At twisted graphene sites
1438	-OH	Deformation of –OH
1399	-OH	Deformations of phenol or conjugated –C-O groups (lactones)
1210	-C-O-R	Unspecific for all single bonded oxo groups

Comparison of band frequencies between different samples and with literature data such as in Table 3 are hampered by the fact that neighbourhood effects and the degree of wetting by moisture from the gas phase or from KBr may lead to considerable shifts (up to 30 cm-1 in the fingerprint region, much larger for the –OH valence region) and line broadening of the sub-patterns for polar groups (most drastically for the –OH groups). For in-depth studies the definition of the hydration state and the thermal history of all samples must thus be defined and kept constant with great reproducibility.
In selected cases EPR spectroscopy can give insight into stable surface radical structures and oxygen species adsorbed thereon (“peroxides”) [95]. The method is very sensitive and quite selective, “sees” however, only a small fraction of all relevant surface functional groups and has thus to be applied only in combination with other chemical and quantitative methods.

An instrumental method suitable for the analysis of a wide range of sample qualities and application purposes is XPS X-ray photoelecton spectroscopy [96,60,97,72] of

carbon. This method has been extensively developed with oxo-functionalising of polymers from where a set of consistent peak assignments can be derived. A compilation of chemical shift data relative to that of defect-free graphite (284.6 eV) is given in Table 4. From these data it occurs that the general rule of chemical shift interpretation for XPS in compounds of main group elements holds here: ground state electrostatic core hole screening is the dominant factor of oxo-functional groups. The stronger the carbon – oxygen interaction the larger is the C 1s shift. A caveat must be put, however, on interpreting small shifts near the main line [98] (shift data below 1.0 eV) as there an additional influence of the electronic structure of the carbon bulk affecting the shape of the main line has to be taken into account. This underlying effect of the electronic structure of the bulk carbon [99] is reflected in the absolute positions of characteristic lines for the same type of functional groups on different substrates as seen in Table 4.

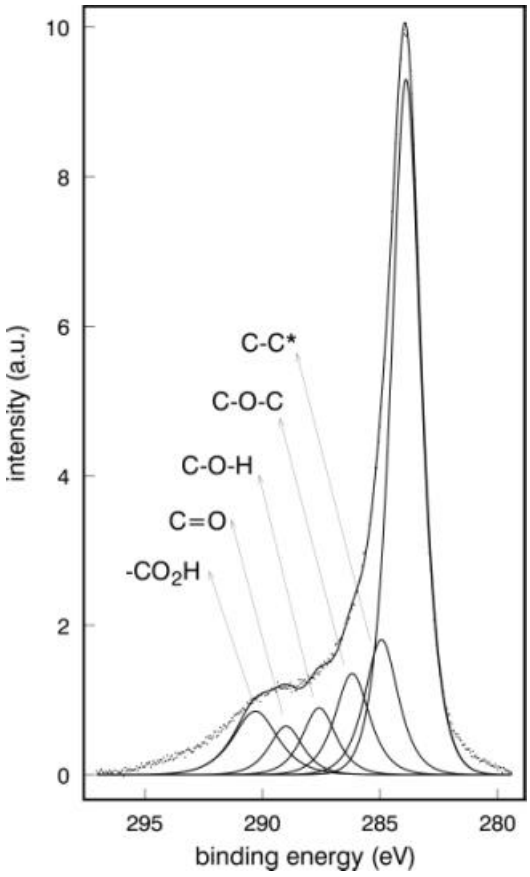

Figure 15: Carbon 1s X-ray photoelectron spectrum of an activated carbon (Norit). The raw data dots are superimposed by non-constrained deconvolution into a minimum (width 2.2 eV) of peaks with Gauss-Lorentz shape. Note: peak widths above ca. 2.7 eV are unphysical.

It should further be noted that XPS is not a highly surface-sensitive technique and with the low-density of valence electrons of graphite a significant escape depth of up to 50 nm must be taken into account. Heteroatoms incorporated at the inner interfaces and within the graphene sheets may thus contribute significantly to the overall spectrum. Surface modifications may thus change the spectral shapes to a small extent only and precision analysis is required the more, the larger is the total content in heteroatoms of a sample. An elegant way out of this intrinsic poor sensitivity is the derivatisation of chemically functional groups by cation exchange such as with Ba exhibiting a high cross section in XPS and being certainly no component of the bulk sample [100].

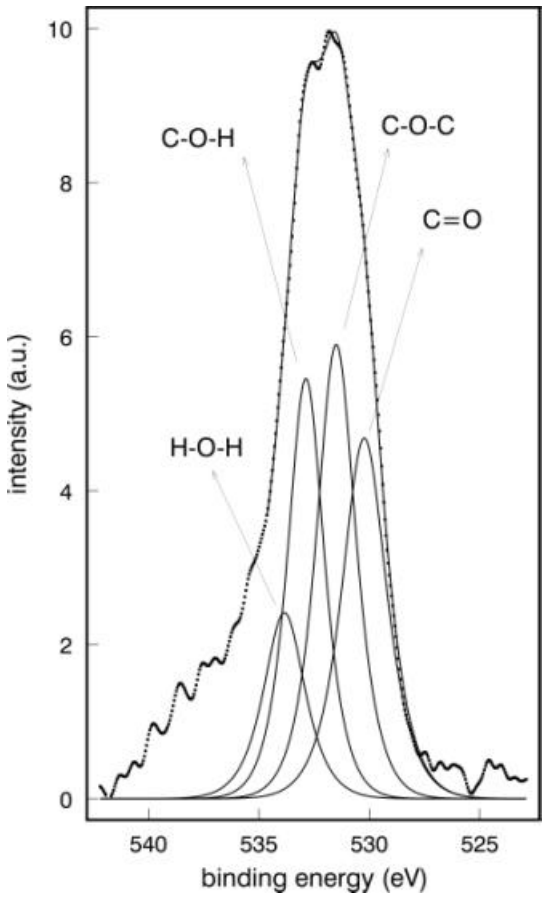

Figure 16: Oxygen 1s photoelectron spectrum of the Norit sample used in Figure 15.

A characteristic example of a complex case is presented in Figures 15 and 16. The carbon 1s spectrum of an activated charcoal (Norit, commercial quality) is shown in Figure 15, Figure 16 reports the corresponding oxygen 1s spectrum. The carbon is analysed in its as-delivered state without any thermal or chemical pre-treatment. The graphitic character of the basic structural units is low, a description of a highly defective sp^2-sp^3 polymer with significant heteroatomic content is more appropriate for this material stemming from biological precursors. Correspondingly a sharp C1s main line with a weak tailing to higher binding energy is observed (Figure 15). This allows to conclude that only a weak structure for the graphitic surface plasmon giving rise to a peak at 291.5 eV in well-crystalline graphite can be expected. Consequently, the whole spectral weight above 285 eV should go to carbon-heteroatom bonds. This is in conflict with data in Table 4 reporting no shifts above 291 eV. The explanation is surface differential charging: parts of the material within

the information depth of XPS (here as much as 80 nm) is insulating in its electronic structure due to poor graphitisation and to high heteroatom content (more an organic macromolecule than carbon). This part of the spectrum cannot be analysed and is hence omitted in the deconvolution procedure. Proof for this comes also from the line profile of the O1s emission shown in Figure 17 where also part of the spectral weight is positioned at high relative energies outside of any chemical shift range.

The deconvolution with Gauss-Lorentz peak profiles yields 5 contributions which can be assigned according to the data in Table 4. This carbon should exhibit a high abundance of strongly acidic surface groups which are thermo labile. The reaction in water is indeed with pH = 3.6 strongly acidic. The assignment of the carbon shifts must also be reflected in the oxygen spectral weight which is well compatible with the analysis of the carbon chemical shifts. Due to the high hydrophilicity and the extensive micro porosity a substantial contribution is detected from molecular water occurring at 533.5 eV. In non-porous carbons this species would be pumped off in the UHV of the spectrometer. The relative abundances of the species in the O 1s spectrum came out from the deconvolution in the same sequence as seen in the carbon 1s line without any constraint in the fitting procedure on the intensity contribution.

Table 4 XPS binding energies of functionalised carbon surafces. All values are relative to the centre of gravity of the graphite C 1s line at 284.6 eV. All values are given in eV.

Surface	C 1s shift	Assignment
Hydrogenated carbon	0.5	C-H
sp^2/sp^3 defective carbon	0.3	C-C defects
Polyvinyl alcohol	1.0	C-O-C
	1.9	C-OH
	3.2	C=O
	4.6	CO_2H
Polyethylene oxidized	1.6	C-O-C
	2.9	C=O
	4.4	CO_2H
Graphite fibre oxidized with HNO_3	1.5	C-OH
	3.0	C=O
	4.5	CO_2H
	5.1	CO_3^{2-}

If the bulk carbon material is graphitic in nature the determination of surface functional groups is severely hampered by the anisotropy of the C 1s line. This anisotropy is caused by a coupling of the core hole to the valence band structure of the semi metallic graphite via a fast relaxation mechanism. The anisotropy of the main line is thus a direct measure of the extent of graphitisation of a carbon material. An illustration is given in Figure 17. Here the spectra of highly oriented pyrolytic graphite (HOPG) representing a single crystal of graphite in the (0001) orientation is compared to the spectrum of graphite nanofilaments [101] with significant amounts of oxygen functional groups. These groups and a contribution from lattice defects become apparent by subtracting the HOPG reference spectrum from that of the sample of interest. The residuum displayed in the inset reveals strongly acidic oxygen function overlapping in the original spectrum strongly with the surface plasmon of graphite at above 291 eV, a contribution from C-O-H groups and also a significant abundance of defective carbon sites with either C-H terminations or sp^3 centres both giving rise to the symmetric broadening recognised in the residuum as symmetric flanks around the zero contribution from the graphite main line.

The surface analysis of carbons deposited at catalytic surfaces such as on metal particles is the only method to learn about functionalisation of traces of adventitious carbon. A combination of XPS data calibrated with the results discussed above and of ultraviolet photoemission was found to be a powerful method to unravel a similar complexity of C-H and C-O-H functions as occurring on bulk samples [102,103].

A versatile and often used [85,44,104] physical method for analysing oxygen functional groups is the temperature-programmed decomposition of the functionalised surface in inert gas or in high vacuum. As result of this destructive treatment a stream of evolved gases containing CO, CO_2 H_20 and eventually CH_4 will result which can be analysed by a variety of techniques ranging from dispersive or non-dispersive infrared spectroscopy over mass spectrometry to gas chromatography. As conceptually simple this analysis may look (and hence as often it is used) as severe are some of its limitations.

Technical limitations relate to the problem of applying an exactly linear temperature ramp to exactly all of the carbon material. For loose powders in tubes or baskets of thermobalances this is not fulfilled giving rise to extra peaks, broadenings and peak structures of erroneous nature and hence leading to the apparent identification of many more species than are actually present. In this context the habit to fit Gaussian lines under broad profiles must be considered with great care as experimental artefacts are much more likely causes for wide desorption profiles than chemically differing species. Another technical problem is the high temperature required to remove the strongly held basic groups which desorb often around 1000 K. At such temperatures the carrier gas and the apparatus must fulfil utmost requirements in cleanliness and air tightness as traces of oxygen or water will initiate bulk gasification which gives rise to very large signals compared to the surface desorption. More fundamental are the following limitations. With all porous samples a significant amount of adsorbed and stored air/water is introduced into the analysis system desorbing only at high temperatures where these traces initiate the reformation of new surface groups and/or even the bulk gasification. The same holds also for large amounts of desorbing surface functional groups giving rise to peaks in the partial pressures of reactive gases which can re-adsorb and produce new groups. Finally, also the thermal load may well restructure functional groups before they desorb as different groups than were initially present. This is true in particular

for basic groups which transform at high temperatures into new more stable and hence apparently non-reactive structures. All these limitations give a rather dynamical and not necessarily representative picture of the distribution of functional groups of a carbon material. The more acidic the groups are the more unstable are they (see section 2) and hence the lower will be the desorption temperature giving rise to less restructuring. Low-temperature spectra up to ca. 800K yield thus more reliable chemical interpretations than high temperature analytical data which are often used, however, with more engineering type characterisations of technical carbons.

An illustration for the analysis of a strongly functionalised carbon is given in Figure 18. The special mass spectrometer (IMR-MS) [105] allows a highly sensitive evolved gas analysis as it does not detect the carrier gas nitrogen. The material contains only few micropores and hence looses at low temperatures adsorbed water. At 400 K the decomposition of strongly acidic carboxyl groups give rise to burst of CO_2 and water. At higher temperatures less-acidic groups containing –OH functions decompose between 600 K and 750 K chemically inert but relatively labile groups give rise to strong CO_2 evolutions. At above 750 K the desorption of more basic and inert (stable) oxygen groups cause the evolution of CO. The fall off in CO_2 is a quality sign of the absence of bulk gasification by leaking or impurity oxygen gas. The very small signal of methane reveals also the existence a small fraction of labile C-H terminations. The decomposition of highly abundant inert C-H groups occurs only at much higher temperatures than applied in this experiment. Great care has to be applied to separate fragmentation in conventional mass spectrometers and the desorption of CO from the filament of the mass spectrometer from the genuine CO evolution curve which should start close to zero for all air-exposed carbon samples. This pattern is typical for many carbon materials.

The fact that the CO_2 evolution starts with such a steep rise indicates a homogeneous and linear heating of the sample. Broad rising low-temperature flanks always should be regarded as indications for technical problems with heat transfer. In turn, the broad emission profile for CO_2 also indicates the wide distribution of oxygen functionalities as discussed in sections 2 and 3. The chemically active part of these groups may be estimated from the concomitant emission of water from –OH groups. This comparison favourably compares with the chemical discrimination discussed with Figure 9.

The reactive oxygen functions were considered so far mainly in the context of acid-base reactions. Oxygen groups can, however, also be of redox chemical function as briefly discussed above. Thermal analysis coupled with isotope labelling experiments can resolve elegantly the speciation problem. A case study is shown in Figure 19. A technical carbon black (Printex 1) was functionalised with NO at atmospheric pressure and at 773 K. This gives rise to few labile acidic functional groups (too high in treatment temperature) but stores significant amounts of non acidic oxygen groups in the sample. This can be identified by a temperature-programmed isotope exchange experiment by heating the sample in low-pressure environment of $^{18}O_2$ and observing subsequently the desorption of previously exchanged oxygen functions under vacuum in the mass channels indicative of isotope exchange (m/e 30 for labelled CO and m/e 46,48 for singly and doubly labelled CO_2). The NO treatment is known to leave C-N functions at the carbon desorbing as N_2, and N_2O. To discriminate N-species from O-species the fragmentation peak ratio m/e 14 for –N and m/e 16 for –O can be used.

The data of Figure 19 indicate the following: Nitrogen is incorporated at the surface (peak at 6000 K) and in various structures within the graphene units (broad feature). The surface desorption occurs together with the liberation of CO_2 which is not or only little labelled indicating that the surface defect holding the nitrogen is chemically stable. A range of redox-active, highly oxygenated functions resulted from the NO decomposition as indicated by the labelled signals occurring at 1000 K. These groups do not hold nitrogen from the initial NO functionalisation indicating surface mobility of the initial fragments ending at different locations from where they were formed. Their structures fall at least in two categories as can be seen from the peak shifts between CO and CO_2 desorption on one hand and the discrimination between singly and doubly labelled CO_2 on the other hand. Chemically non-reactive groups desorb above 950 K as CO and in a sharp emission at 1080 K as CO_2 indicating that also the non-reactive groups occur in different structures.

In conclusion it occurs from the examples as well as from the general comments about the methodologies that the speciation of carbon surface functional groups is a difficult task if structural resolution is required. Only combinations of physical and chemical methods provide sufficient overview. Great care has to be taken to discriminate reactive and non-reactive species. The reactivity has to be evaluated in terms of acid-base and redox functionality which address different sub-sets of all oxygen functional groups present. The enormous variation in local structure and the unlimited combination of all functions at the surface provide a chameleon-like behaviour of many carbon materials responding as single material to their varying environment in different ways.

References

(1) Schlögl, R. Carbons In Handbook of Heterogeneous Catalysis; G. Ertl, H. Knözinger, J. Weitkamp, Eds.; VCH Verlagsgesellschaft: Weinheim, 1997; Vol. 1, Chapter 2.1.9; pp 138-191.
(2) Janoschek, R. Chemie i. u. Zeit 1988, 4 , 128-138.
(3) Whittaker, A. G. and Kintner, P. L. Science 1969, 165 (8) , 589-591.
(4) Charlier, J.-C.; Michenaud, J.-P. and Lambin, P. Phys. Rev. B 1992, 46 (8) , 4540-4543.
(5) Fitzgerald, J. D.; Taylor, G. H.; Brunckhorst, L. F.; Pang, L. S. K.; Terrones, M. H. and Mackay, A. L. Carbon 1992, 30 , 1251-1260.

(6) Kroto, H. Science 1988, 242 , 1139-1145.
(7) Marchon, B. and Salmeron, M. Phys. Rev. B 1989, 39 (17) , 12907-12910.
(8) Elings, V. and Wudl, F. J. Vac. Sci. Technol. 1988, A 6 (2) , 412-414.
(9) McFeely, F. R.; Kowalczyk, S. P.; Ley, L.; Cavell, R. G.; Pollak, R. A. and Shirley, D. A. Phy. Rev. B 1974, 9 (12) , 5268-5278.
(10) Terrones, H. Mackay, A.L.; Chem. Phys. Lett. 1993, 207, 45-50.
(11) Kincaid, B. M.; Meixner, A. E. and Platzman, P. M. Phys. Rev. B 1978, 40 (19) , 1296-1299.
(12) Atamny, F.; Blöcker, J.; Henschke, B.; Schlögl, R.; Schedel-Niedrig, T.; Keil, M. and Bradshaw, A. M. J. Phys. Chem. 1992, 96 , 4522.
(13) Belton, D. N. and Schmieg, S. J. J. Vac. Sci. Technol. 1990, A 8 (3) , 2353-2362.
(14) Ugolini, D.; Eitle, J.; Oelhafen, P. and Wittmer, M. Appl. Phys. 1989, A 48 , 549-558.
(15) Engel, W.; Ingram, D. C.; Keay, J. C. and Kordesch, M. E. Diamond and Related Materials 1994, 3 , 1227-1229.
(16) Kyotani, T. Carbon 2000, 38 (2) , 269-286.
(17) Nicholson, A. P. P. and Bacon, D. J. Carbon 1974, 13 , 275-282.
(18) Amelinckx, S.; Delavignette, P. and Heerschap, M. Chem. Phys. Carbon 1965, 1 , 2.
(19) Chu, X. and Schmidt, L. D. Ind. Eng. Chem. Res. 1993, 32 , 1359-1366.
(20) Thomas, J. M. Chem. Phys. Carbon 1965, 1 , 121.
(21) Studebaker, M. L. Rubber Chem. Technol. 1957, 30 , 1400-1483.
(22) Audier, M.; Oberlin, A.; Coulon, M. and Bonnetain, L. Carbon 1981, 19 , 217-224.
(23) Miki-Yoshida, M.; Catillo, R.; Ramos, S.; Rendón, L.; Tehuycanero, S.; Zou, B. S. and José-Yacamán, M. Carbon 1994, 32 (2) , 231-246.
(24) Oberlin, A. Chem. Phys. Carbon 1992, 22 , 2.
(25) Rostrup-Nielsen, J. R. J. Catal. 1972, 27 , 343-356.
(26) Baker, R. T. K. Amer. Chem. Soc., Fuel Chem. 1996, 41 (2) , 521-524.
(27) Davis, S. M.; Zaera, F. and Somorjai, G. A. J. Catal. 1982, 77 , 439-459.
(28) van Doorn, J. and Moulijn, J. A. Catal. Today 1990, 7 , 257-266.
(29) Albers, P.; Bösing, S.; Prescher, G.; Seibold, K.; Ross, D. K. and Parker, S. F. Appl. Catal. A: General 1999, 187 , 233-243.
(30) Homann, K. H. and Wagner, H. G. Proc. Roy. Soc. A 1968, 307 , 141-152.
(31) Frenklach, M. and Ebert, L. B. J. Phys. Chem. 1988, 92 , 563-564.
(32) Lahaye, J.; Prado, G. Mechanisms of Carbon Black Formation In Chemistry and Physics of Carbon; P. L. Walker jr., P. A. Thrower, Eds.; Marcel Dekker, 1978; Vol. 14; pp 167-294.
(33) Becker, A. and Hüttinger, K. J. Carbon 1998, 36 (3) , 177-199.
(34) Bonnetain, L.; Duval, X.; Letort, M. In Proc. 4th Carbon Conf., Buffalo; Pergamon Press, 1960; pp 107-112.
(35) Delannay, F.; Tysoe, W. T.; Heinemann, H. and Somorjai, G. A. Carbon 1984, 22 (4/5) , 401-407.
(36) Kelemen, S. R.; Freund, H. and Mims, C. A. J. Catal. 1986, 97 , 228-239.
(37) Schlögl, R.; Loose, G. and Wesemann, M. Solid State Ionics 1990, 43 , 183-192.
(38) Henschke, B.; Schubert, H.; Blöcker, J.; Atamn y, F. and Schlögl, R. Thermochim. Acta 1994, 234 , 53-83.
(39) Marsh, H.; O'Hair, T. E. and Wynne-Jones, W. F. K. Trans. Faraday Soc. 1965, 61 , 274-283.
(40) You, H.; Brown, N. M. D.; Al-Assadi, K. F. and Meenan, B. J. J. Mater. Sci. 1993, 12 , 201-204.
(41) Atamny, F.; Blöcker, J.; Dübotzky, A.; Kurt, H.; Loose, G.; Mahdi, W.; Timpe, O. and Schlögl, R. J. Mol. Phys. 1992, 76 (4) , 851-886.
(42) Zhuang, Q.; Kyotani, T. and Tomita, A. Energy & Fuels 1995, 9 , 630-634.
(43) Vastola, F. J.; Hart, P. J. and Walker, P. L. Carbon 1964, 2 , 65-71.
(44) Moulijn, J. A. and Kapteijn, F. Carbon 1995, 33 (8) , 1155-1165.
(45) Carzorla-Amorós, D.; Linares-Solano, A.; Dekker, F. H. M. and Kapteijn, F. Carbon 1995, 33 (8) , 1147-1154.
(46) Ismail, I. M. K. and Walker jr., P. L. Carbon 1989, 27 (4) , 549-559.
(47) Lizzio, A. A.; Jiang, H. and Radovic, L. R. Carbon 1990, 28 , 7-19.
(48) Werner, H.; Schedel-Niedrig, T.; Wohlers, M.; Herein, D.; Herzog, B.; Schlögl, R.; Keil, M.; Bradshaw, A. M. and Kirschner, J. J. Chem. Soc. Farad. Trans. 1994, 90 (3) , 403-409.
(49) Chen, H. S.; Kortan, A. R.; Haddon, R. C.; Kaplan, M. L.; Chen, C. H.; Mujsce, A. M.; chou, H. and Fleming, D. A. Appl. Phys. Lett. 1991, 59 (23) , 2956.
(50) Boehm, H. P.; Bewer, G. In Proc. 4th Internat. Conf. Carbon and Graphite; Soc. Chem. Int., Ed.: London, 1974; pp 344-359.
(51) Yang, J.; Herein, D.; Mestl, G.; Schlögl, R. and Find, J. Carbon 2000, 38 (5) , 715-727.
(52) Stöhr, B.; Boehm, H. P. and Schlögl, R. Carbon 1991, 29 (6) , 707-720.
(53) Pels, J. R.; Kapteijn, F.; Moulijn, J. A.; Zhu, Y. and Thomas, K. M. Carbon 1995, 33 (11) , 1641-1653.
(54) Evans, E. L.; Lopez-Gonzalez, J. d. D.; Martin-Rodriguez, A. and Rodriguez-Reinoso, F. Carbon 1975, 13 , 461-464.
(55) Boehm, H. P.; Mair, G.; Stöhr, T. In 17th Bienn. Conf. on Carbon; / Lexington, 1985; pp 381-382.
(56) Kürpick, U.; Meister, G. and Goldmann, A. Appl. Phys. A 1992, 55 , 529-532.
(57) Bansal, R. C.; Dhami, T. L. and Parkash, S. Carbon 1977, 15 , 157-160.
(58) Bansal, R. C.; Vastola, F. J. and Walker, P. L. Carbon 1971, 9 , 185-192.
(59) Arico, A. S.; Antonucci, V.; Minutoli, M. and Giordano, N. Carbon 1989, 27 (3) , 337-347.
(60) Kozlowski, C. and Sherwood, P. M. A. J. Cem. Soc., Faraday Trans. I 1985, 81 , 2745-2756.
(61) Boehm, H.-P. Angew. Chem. 1966, 78 (12) , 617-628.
(62) Marsh, H.; Foord, A. D.; Mattson, J. S.; Thomas, J. M. and Evans, E. L. J. Colloid Interface Sci. 1974, 49 (3) , 368-382.
(63) Bansal, R. C.; Vastola, F. J. and Walker jr., P. L. J. Colloid Interface Sci. 1970, 32 (2) , 187-194.
(64) Rodriguez-Reinoso, F. Carbon 1998, 36 (3) , 159-175.
(65) Boehm, H.-P. and Diehl, E. Z. Electrochem. 1962, 66 (8/9) , 642-647.
(66) Boehm, H. P. Adv. Catal. 1966, 16 , 179-274.
(67) Papirer, E.; Li, S. and Donnet, J.-B. Carbon 1987, 25 (2) , 243-247.
(68) Garten, V. A. and Weiss, D. E. Aust. J. Chem. 1957, 10 , 309-328.
(69) Boehm, H.-P. and Voll, M. Carbon 1970, 8 , 227-240.
(70) Ismail, I. M. K. and Rodgers, S. L. Carbon 1992, 30 (2) , 229-239.
(71) Werner, H.; Wohlers, M.; Bublak, D.; Belz, T.; Bensch, W.; Schlögl, R. In Electronic Properties of Fullerenes; H. Kuzmany, J. Fink, M. Mehring, Eds.; Springer Series in Solid State Sciences, 1993; Vol. 117; pp 16-38.
(72) Burmeister, R.; Despeyroux, B.; Deller, K.; Seibold, K. and Albers, P. Stud. Surf. Sci. Catal. 1993, 78 , 361-368.
(73) Moreno-Castilla, C.; Salas-Peregrin, M. A. and López-Garzón, F. J. Fuel 1995, 74 (6) , 830-835.
(74) Hegenberger, E.; Wu, N. L. and Phillips, J. J. Phys. Chem. 1987, 91 , 5067-5071.
(75) Weng, L. T.; Poleunis, C.; Bertrand, P.; Carlier, V.; Sclavons, M.; Franquinet, P. and Legras, R. J. Adhesion Sci. Technol. 1995, 9 (7) , 859-871.
(76) Wu, G. M.; Schultz, J. M.; Hodge, D. J. and Cogswell, F. N. Polymer Composites 1995, 16 (4) , 284-287.

(77) Zielke, U.; Hüttinger, K. J. and Hoffman, W. P. Carbon 1996, 34 (8) , 999-1005.
(78) Zielke, U.; Hüttinger, K. J. and Hoffman, W. P. Carbon 1996, 34 (8) , 1007-1013.
(79) Bandosz, T. J.; Jagiello, J.; Contescu, C. and Schwarz, J. A. Carbon 1993, 31 (7) , 1193-1202.
(80) Belz, T.; Find, J.; Herein, D.; Pfänder, N.; Rühle, T.; Werner, H.; Wohlers, M. and Schlögl, R. Ber. Bunsenges. Phys. Chem. 1997, 101 (4) , 712-725.
(81) Hofmann, U. and Ohlerich, G. Angew. Chem. 1950, 62 (1) , 16-21.
(82) Boehm, H.-P.; Diehl, E.; Heck, W. and Sappok, R. Angew. Chem. 1964, 76 (17) , 742-751.
(83) Stacy, W. O.; Imperial, W. R. and Walker, P. L. Carbon 1966, 4 , 343-352.
(84) Jansen, R. J. J. and Bekkum, H. v. Carbon 1995, 33 , 1021-1027.
(85) Voll, M. and Boehm, H.-P. Carbon 1970, 8 , 741-752.
(86) Voll, M. and Boehm, H.-P. Carbon 1971, 9 , 473-480.
(87) Voll, M. and Boehm, H.-P. Carbon 1971, 9 , 481-488.
(88) Ehrburger, P.; Mahajan, O. P. and Walker jr., P. L. J. Catal. 1976, 43 , 61-67.
(89) Groszek, A. J. Carbon 1987, 25 (6) , 717-722.
(90) Papirer, E. and Guyon, E. Carbon 1978, 16 , 127-131.
(91) Garten, V. A. and Weiss, D. E. Rev. of Pure and Appl. Chem. 1957, 7 , 69-123.
(92) Yang, Y. and Lin, Z. G. J. Appl. Electrochem. 1995, 25 , 259-266.
(93) Zawadzki, J. In Chemistry and Physics of Carbon; P. A. Thrower, Ed.; Marcel Dekker Inc., 1989; Vol. 21.
(94) O'Reilly, J. M. and Mosher, R. A. Carbon 1983, 21 (1) , 47-51.
(95) Watanabe, A.; Ishikawa, H.; Mori, K. and Ito, O. Carbon 1989, 27 (6) , 863-867.
(96) Wild, U.; Pfänder, N. and Schlögl, R. Fresenius J. Anal. Chem. 1997, 357 (4) , 420-428.
(97) Takahagi, T. and Ishitani, A. Carbon 1988, 26 (3) , 389-396.
(98) Schlögl, R. and Boehm, H. P. Carbon 1983, 21 (4) , 345-358.
(99) Baer, Y. J. Electr. Spectrosc. Rel. Phen. 1981, 24 , 95-100.
(100) Denison, P.; Jones, F. R. and Watts, J. F. J. Mater. Sci. 1985, 20 , 4647-4656.
(101) Belz, T.; Bauer, A.; Find, J.; Günter, M.; Herein, D.; Möckel, H.; Pfänder, N.; Sauer, H.; Schulz, G.; Schütze, J.; Timpe, O.; Wild, U. and Schlögl, R. Carbon 1998, 36 (5-6) , 731-741.
(102) Paál, Z.; Wootsch, A.; Matusek, K.; Wild, U. and Schlögl, R. Catal. Today 2000, 2264 , 1-6.
(103) Rodriguez, N. M. ,. A. P. E.; Wootsch, A.; Wild, U.; Schlögl, R. and Paál, Z. J. Catal. 2001, 197 , 365-377.
(104) Kapteijn, F.; Meier, R.; van Eyck, S. C.; Moulijn, J. A. / Fundamental Issues in Control of Carbon Gasification; J. Lahaye, P. Ehrburger, Eds.; Kluver, 1991; p 221.
(105) Bassi, D.; Tosi, P. and Schlögl, R. J. Vac. Sci. Technol. A 1998, 16 (1) , 114-122.